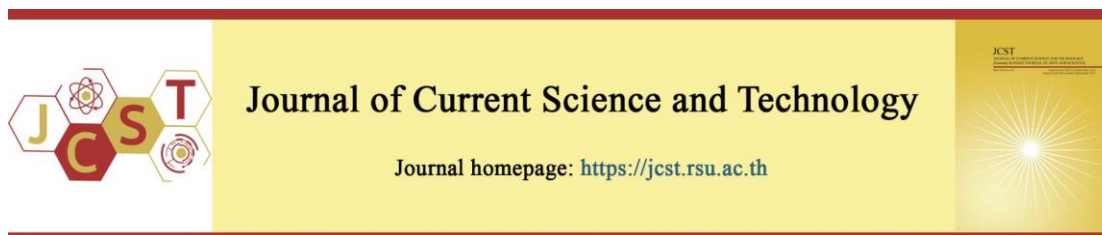


Cite this article: Kumari, P., & Sharma, B. S. (2021, September). Hot carrier effects on real and imaginary parts of Brillouin susceptibilities of semiconductor magneto-plasmas. *Journal of Current Science and Technology*, 11(3), 411-423. DOI: 10.14456/jcst.2021.41



Hot carrier effects on real and imaginary parts of Brillouin susceptibilities of semiconductor magneto-plasmas

Pinki Kumari* and B.S. Sharma

Department of Physics, Lords University, Chikani, Alwar – 301028 (Rajasthan) India

*Corresponding author; E-mail: pinki.lordsuniv@gmail.com

Received 21 July 2021; Revised 28 July 2021; Accepted 14 August 2021;
Published online 28 September 2021

Abstract

An analytical investigation is made of hot carrier effects on real and imaginary parts of Brillouin susceptibility ($\text{Re}(\chi_B)$, $\text{Im}(\chi_B)$) of semiconductor magneto-plasmas. Coupled mode approach is used to obtain expressions for ($\text{Re}(\chi_B)$ and $\text{Im}(\chi_B)$). Numerical calculations are made for n-InSb crystal – CO₂ laser system. Efforts are made to obtain enhanced values of ($\text{Re}(\chi_B)$ and $\text{Im}(\chi_B)$) as well as change of their sign under appropriate selection of external magnetic field (B_0) and doping concentration (n_0). The hot carrier effects of intense laser radiation modifies the momentum transfer collision frequency of carriers and consequently the nonlinearity of the medium, which in turn (i) further enhances ($\text{Re}(\chi_B)$ and $\text{Im}(\chi_B)$), (ii) shifts the enhanced ($\text{Re}(\chi_B)$ and $\text{Im}(\chi_B)$) towards smaller values of B_0 , and (iii) widens the range of B_0 at which change of sign of ($\text{Re}(\chi_B)$ and $\text{Im}(\chi_B)$) occur. The change of sign of enhanced ($\text{Re}(\chi_B)$ and $\text{Im}(\chi_B)$) of semiconductor magneto-plasmas validates the possibility of chosen Brillouin medium as a potential candidate material for the fabrication of stimulated Brillouin scattering dependent widely tunable and efficient optoelectronic devices such as optical switches and frequency converters.

Keywords: Brillouin susceptibility; hot carrier effects; laser-plasma interactions; magnetic field; semiconductor magneto-plasmas.

1. Introduction

The study of nonlinear optical susceptibility provides an important information of the nonlinearity of a medium and imparts an extensive role in the fabrication of optoelectronic devices (Säynätjoki et al., 2017; Sharaf, Mohammed, Zahran, & Shaaban, 2021; You, Bongu, Bao, & Panoiu, 2018). In addition, the change of sign of nonlinear optical susceptibility exhibits interesting nonlinear optical phenomena (Takeya, Kamei, Kawase & Uchida, 2020; Lu, Zhang, Wu, Chen, & Xu 2021; Wang et al., 2021). The selection and operating frequency of a medium are the essential features used in designing the optoelectronic devices. Out of various nonlinear media, the semiconductor plasmas offer greater flexibility in fabrication of optoelectronic devices.

This is due to their compactness, provision of control of (electrons/holes) carriers relaxation time via materials designing and device structuring, operation of the devices under oblique/normal incidence or in waveguide structures, highly advanced fabrication technology, and integrating the devices with other optoelectronic components (Mokkapatil & Jagadish, 2009). In addition, these media exhibit large nonlinear optical susceptibility in close proximity to the band-gap resonant transition regimes, which can be further enhanced by application of external electric/magnetic fields (Sandeep, Dahiya, & Singh, 2017; Bhan, Singh Kumar & Singh, 2019; Singh, Gahlawat, Sangwan, Singh, & Singh, 2020). Thus, the selection of semiconductor-plasma as nonlinear media for the

study of nonlinear optical phenomena is unquestionable.

Out of various nonlinear optical phenomena, the study of stimulated Brillouin scattering (SBS) is currently a major field of research due to its vast potentiality over a broad range of optoelectronic devices (Garmire, 2017; Bai et al., 2018). SBS occurs due to scattering of a laser radiation by an internally generated acoustical vibrational mode of the medium. It is a third-order optical phenomenon and its origin lies in third-order (Brillouin) susceptibility of the medium. In the past, Brillouin susceptibility of semiconductor magneto-plasmas has been widely explored to study SBS and related phenomena (Singh & Aghamkar, 2008; Singh, Aghamkar, Kishore, & Sen, 2008; Uzma, Zeba, Shah, & Salimullah, 2009; Vanshpal, Dubey, & Ghosh, 2013; Sharma, Dad, & Ghosh, 2015). Keeping in mind the overall performance of SBS based optoelectronic devices, the knowledge of Brillouin susceptibility of semiconductor plasmas as well as its characteristic dependence on various affecting factors is essential (Garmire, 2018).

Literature survey reveals that no theoretical formulation has been made till now to explore the influence of hot carrier effects (HCEs) on Brillouin susceptibility in semiconductor plasmas. In the present paper, we developed a theoretical formulation followed by numerical analysis to study HCEs of intense laser radiation on real and imaginary parts of Brillouin susceptibility of semiconductor magneto-plasmas (acting as Brillouin media). The motivation for this study arises from the fact that HCEs of intense laser radiation may remarkably modify the nonlinearity of the medium and consequently the SBS phenomenon. Under high-power laser irradiation, this investigation becomes more important as it leads to better understanding of SBS phenomenon in semiconductor magneto-plasmas. Considering the origin of the phenomenon to lie in finite nonlinear induced polarization (arising due to coupling between internally generated acoustical vibrational mode and laser radiation field) and using the coupled mode theory of interacting waves, expressions are obtained for real and imaginary parts of Brillouin susceptibility of semiconductor magneto-plasmas under hydrodynamic approximation. Efforts are made to optimize the doping level and to find appropriate values of external magnetic field to enhance magnitude of

real and imaginary parts Brillouin susceptibility as well as alter of their sign for applications in efficient optoelectronic devices, such as optical switches, frequency converters. Finally, complete numerical analysis is made with a set of data available for n -InSb illuminated by a pulsed CO₂ laser.

2. Objectives

The objective of the present analytical investigation is to study HCEs on real and imaginary parts of Brillouin susceptibility of semiconductor magneto-plasmas. Efforts are directed towards to determine appropriate values of doping concentration and external magnetic field to enhance the magnitude of real and imaginary parts Brillouin susceptibility, change of their sign, and to establish the suitability of semiconductor magneto-plasmas as hosts for fabrication of efficient optoelectronic devices.

3. Theoretical formulations

In this section, expressions are obtained for real and imaginary parts of Brillouin susceptibility ($\text{Re}(\chi_B)$, $\text{Im}(\chi_B)$) of semiconductor magneto-plasmas under hydrodynamic approximation: $k_a l \ll 1$, where is k_a the acoustical vibrational wave number, and l is the carriers mean free path (Chefranov & Chefranov, 2020).

In high density semiconductor plasmas, because of the inter-fermion distances much smaller than the de-Broglie wavelength of plasma particles and the influence of Pauli exclusion rule, a lot of quantum effects may arise (Rasheed, Jamil, Siddique, Huda, & Jung, 2014). The variations in linear and nonlinear responses of quantum semiconductor plasmas from that of classical ones have been reported (Moghanjoughi, 2011). Most of these investigations are based on quantum hydrodynamic (QHD) model of semiconductor plasmas. This model is helpful in analytical investigations of the short-scale collective phenomena in high density semiconductor plasmas (Hass & Bret, 2012). By the inclusion of quantum diffraction terms and the statistical degeneracy pressure, QHD model becomes a generalization of the usual fluid model. Using QHD model, the study of hot carrier effects on Brillouin susceptibility in quantum semiconductor magneto-plasmas is our future plan of research work.

In a Brillouin medium, SBS phenomenon occurs due to nonlinear interaction among three

coherent fields in a Brillouin medium, viz. an intense laser radiation field $E_0(x, t) = E_0 \exp[i(k_0 x - \omega_0 t)]$, an induced acoustical vibrational mode $u(x, t) = u_0 \exp[i(k_a x - \omega_a t)]$, and scattered Stokes component of incident laser radiation field $E_s(x, t) = E_s \exp[i(k_s x - \omega_s t)]$. These fields are connected by energy and momentum phase matching constraints $\hbar\omega_0 = \hbar\omega_a + \hbar\omega_s$ and $\hbar\vec{k}_0 = \hbar\vec{k}_a - \hbar\vec{k}_s$, respectively. The Brillouin medium is subjected to an external magnetic field $\vec{B}_0 = \hat{z}B_0$ (i.e. perpendicular to wave vectors \vec{k}_0 , \vec{k}_a and \vec{k}_s). This configuration is known as Voigt geometry (Tuz, Fesenko, Fedorin, Sun, & Han, 2017).

The basic equations used in the formulation of $\text{Re}, \text{Im}(\chi_B)$ are:

$$\frac{\partial^2 u(x, t)}{\partial t^2} = \frac{C}{\rho} \frac{\partial^2 u(x, t)}{\partial x^2} - 2\Gamma_a \frac{\partial u(x, t)}{\partial t} - \frac{\beta}{\rho} \frac{\partial E_1}{\partial x} + \frac{\gamma}{2\rho} \frac{\partial}{\partial x} (E_0 E_1^*) \quad (1)$$

$$\frac{\partial \vec{v}_0}{\partial t} + v_0 \vec{v}_0 + \left(\vec{v}_0 \cdot \frac{\partial}{\partial x} \right) \vec{v}_0 = -\frac{e}{m} [\vec{E}_0 + (\vec{v}_0 \times \vec{B}_0)] = -\frac{e}{m} (\vec{E}_c) \quad (2)$$

$$\frac{\partial \vec{v}_1}{\partial t} + v_0 \vec{v}_1 + \left(\vec{v}_0 \cdot \frac{\partial}{\partial x} \right) \vec{v}_1 + \left(\vec{v}_1 \cdot \frac{\partial}{\partial x} \right) \vec{v}_0 = -\frac{e}{m} [\vec{E}_1 + (\vec{v}_0 \times \vec{B}_0)] \quad (3)$$

$$\frac{\partial n_1}{\partial t} + n_0 \frac{\partial v_1}{\partial x} + n_1 \frac{\partial v_0}{\partial x} + v_0 \frac{\partial n_1}{\partial x} = 0 \quad (4)$$

$$\vec{P}_{es} = -\gamma \frac{\partial u^*}{\partial x} (\vec{E}_0) \quad (5)$$

$$\frac{\partial E_1}{\partial x} + \frac{\beta}{\varepsilon} \frac{\partial^2 u}{\partial x^2} + \frac{\gamma}{\varepsilon} \frac{\partial^2 u^*}{\partial x^2} (E_0) = -\frac{n_1 e}{\varepsilon} \quad (6)$$

These equations have been used in analytical investigation of SBS in semiconductor plasmas (Singh, Aghamkar, Kishore, & Sen, 2006; Singh & Aghamkar, 2008; Singh et al., 2008). Here, C represents the elastic stiffness constant of the Brillouin medium such that the speed of acoustical vibrational mode is given by $v_a = (C/\rho)^{1/2}$. ρ is the mass density of Brillouin medium. In order to take account of acoustical damping, the term $2\Gamma_a \partial u(x, t)/\partial t$ in Eq. (1) is introduced phenomenologically. In Eq. (1), β and γ represent the piezoelectric and electrostrictive coefficients of the Brillouin medium, respectively. Here, these coefficients are used

phenomenologically; their effect on Brillouin nonlinearity of semiconductor plasmas is available in literature (Singh et al., 2006). E_1 represents the space charge electric field of the Brillouin medium. n_0 (\vec{v}_0) and n_1 (\vec{v}_1) represent the carrier's (here electrons) equilibrium and perturbed concentrations (oscillatory fluid velocities), respectively. v_0 stands for momentum transfer collision frequency (MTCF) of electrons. m is the effective mass of an electron. P_{es} is the polarization originating via electrostrictive property of the Brillouin medium. The asterisk (*) represents the conjugate of a complex entity.

From Eq. (2), the x - and y -components of equilibrium electron fluid velocity are obtained as:

$$v_{0x} = \frac{e(v + i\omega_0)}{m(\omega_c^2 - \omega_0^2 + 2iv\omega_0)} E_0, \quad (7a)$$

and

$$v_{0y} = \frac{\omega_c}{(v + i\omega_0)} v_{0x}. \quad (7b)$$

In Eqs. (7a) and (7b), $\omega_c = \frac{eB_0}{m}$ is the electron-cyclotron frequency.

From Eq. (2), the x - and y -components of perturbed electron fluid velocity can be obtained from Eq. (3) by using the method adopted by Sharma and Ghosh (2001) as:

$$v_{1x} = \frac{v}{(v^2 + \omega_c^2)} \left[\vec{E} - ik_0 \left(\frac{k_B T_0}{mn_0} \right) n_1 \right], \quad (8a)$$

and

$$v_{1y} = \frac{\omega_c}{(v^2 + \omega_c^2)} \left[-\vec{E} + ik_0 \left(\frac{k_B T_0}{mn_0} \right) n_1 \right]. \quad (8b)$$

In Eqs. (8a) and (8b), $\vec{E} = \frac{e}{m} \langle \vec{E}_c \rangle$, T_0 is the temperature of Brillouin medium, and k_B is the Boltzmann constant.

In order to excite SBS, the fundamental requirement is to irradiate the Brillouin sample by an intense laser. Under the influence of intense laser radiation field, the electrons (which are mobile charge carriers in n -type doped semiconductor) gain energy and their temperature increases to $T_e (> T_0)$. Consequently, the MTCF modifies via relation (Beer, 1963):

$$v = v_0 \left(\frac{T_e}{T_0} \right)^{1/2}. \quad (9)$$

In Eq. (9), the ratio T_e/T_0 can be determined from energy conservation relation under steady-state condition. Following Sodha, Ghatak & Tripathi (1974) and using Eqs. (7a) and (7b), the time independent part of power absorbed by a single electron from the laser radiation field is given by

$$\frac{e}{2} \text{Re}(v_{0x} \cdot \vec{E}_e^*) = \frac{e^2 v_0}{2m} \frac{(\omega_c^2 - \omega_0^2)}{[(\omega_c^2 - \omega_0^2)^2 + 4v_0^2 \omega_0^2]} |\vec{E}_0|^2, \quad (10)$$

where $\text{Re}(v_{0x} \cdot \vec{E}_e^*)$ denotes the real part of the quantity $(v_{0x} \cdot \vec{E}_e^*)$.

Following Conwell (1967), the power dissipated by a single electron from the laser radiation field in collisions with polar optical phonons (POPs) is given by

$$\left(\frac{\partial \epsilon}{\partial t} \right)_{\text{diss}} = e E_{po} (x_0)^{1/2} \kappa_0 \left(\frac{2k_B \theta_D}{m\pi} \right)^{1/2} \left(\frac{x_e}{2} \right) \cdot \exp\left(\frac{x_e}{2}\right) \cdot \frac{\exp(x_0 - x_e) - 1}{\exp(x_0) - 1}, \quad (11)$$

where $x_{0,e} = \frac{h\omega_l}{k_B T_{0,e}}$, in which $h\omega_l (= k_B \theta_D)$ is the energy possessed by POPs, where θ_D is the Debye temperature. $E_{po} = \frac{meh\omega_l}{h^2} \left(\frac{1}{\epsilon_\infty} - \frac{1}{\epsilon} \right)$ represents the POPs scattering potential field, in which ϵ and ϵ_∞ are the static and high frequency dielectric constant of the Brillouin medium, respectively.

Under steady-state condition, the power absorbed by a single electron from the laser radiation field is exactly equal to the power dissipated by it in collisions with POPs. Consequently, the electron-plasma attains a steady temperature T_e . For average heating of the electrons plasma, Eqs. (10) and (11) yield

$$\frac{T_e}{T_0} = 1 + \alpha \left| \frac{\vec{r}}{E_0} \right|^2, \quad (12)$$

where $\alpha = \frac{e^2 v_0}{2m\tau\Omega_0^2} \frac{(\omega_c^2 - \omega_0^2)}{[(\omega_c^2 - \omega_0^2)^2 + 4v_0^2 \omega_0^2]}$, in which

$$\tau = e E_{po} \kappa_0 \left(\frac{2k_B \theta_D}{m\pi} \right)^{1/2} \left(\frac{x_0}{2} \right) \frac{(x_0)^{1/2} \exp(x_0/2)}{\exp(x_0) - 1}.$$

Using Eqs. (9) and (11), the modified MTCF of electrons is given by

$$v = v_0 \left(1 + \alpha \left| \frac{\vec{r}}{E_0} \right|^2 \right)^{1/2} \approx v_0 \left(1 + \frac{1}{2} \alpha \left| \frac{\vec{r}}{E_0} \right|^2 \right). \quad (13)$$

The laser radiation field produces electron density perturbations in the Brillouin medium (via piezoelectric and electrostrictive strains). The coupled equation of these perturbations, including HCEs, can be obtained by using the standard approach (Nimje, Dubey & Ghosh, 2011). Differentiating Eq. (4), substitute the value of E_1 from Eq. (6), first-order derivatives of v_0 and v_1 from Eqs. (2) and (3), respectively and after mathematical simplification, we obtain

$$\frac{\partial^2 n_1}{\partial t^2} + v \frac{\partial n_1}{\partial t} + \bar{\omega}_p^2 n_1 + \frac{n_0 e k_s^2 u^* (\beta \gamma \delta_1 \delta_2 A + \gamma^2 E_0^2)}{m \epsilon_1} E_0 E_s^* = i n_1 k_s \bar{E}, \quad (14)$$

where $A = \frac{\omega_p^2}{(e/m)k_a}$, $\bar{\omega}_p = \frac{v\omega_p}{(v^2 + \omega_c^2)^{1/2}}$, $\delta_1 = 1 - \frac{\omega_c^2}{(\omega_0^2 - \omega_c^2)}$, $\delta_2 = 1 - \frac{\omega_c^2}{(\omega_s^2 - \omega_c^2)}$, and $\omega_p = \left(\frac{n_0 e^2}{m \epsilon} \right)^{1/2}$ (electron-plasma frequency).

The perturbed electron concentration (n_1) may be put forward as: $n_1 = n_{1s}(\omega_a) + n_{1f}(\omega_s)$, where n_{1s} and n_{1f} are known as low- and high-frequency components; oscillate at acoustical vibrational mode frequency ω_a and electromagnetic waves at frequencies $\omega_0 \pm p\omega_a$, in which $p = 1, 2, 3, \dots$, respectively. The electromagnetic fields at sum (i.e. $\omega_0 + p\omega_a$) and difference frequencies (i.e. $\omega_0 - p\omega_a$) are termed as anti-Stokes and Stokes modes, respectively. In the present analysis, the electron density perturbations at off-resonant frequencies (with $p \geq 2$) are neglected and only the first-order Stokes mode (with $p = 1$) is considered (Singh et al., 2008). Under rotating-wave approximation (RWA), Eq. (14) leads to following coupled wave equations:

$$\frac{\partial^2 n_{1f}}{\partial t^2} + v \frac{\partial n_{1f}}{\partial t} + \bar{\omega}_p^2 n_{1f} + \frac{n_0 e k_s^2 u^* (\beta \gamma \delta_1 \delta_2 A + \gamma^2 E_0^2)}{m \epsilon} E_0 E_s^* = -i n_{1s}^* k_s \bar{E} \quad (15a)$$

and

$$\frac{\partial^2 n_{1s}}{\partial t^2} + v \frac{\partial n_{1s}}{\partial t} + \bar{\omega}_p^2 n_{1s} = i n_{1f}^* k_s \bar{E}. \quad (15b)$$

Eqs. (15a) and (15b) manifest that both n_{1s} and n_{1f} are coupled to each other via laser radiation field (\bar{E}). Thus, it clearly illustrates that

the presence of the laser radiation field is the primary requirement for SBS to occur.

Solving Eqs. (15a) and (15b) and using Eq. (1), an expression for n_{1s} may be obtained as:

$$n_{1s} = \frac{\epsilon_0 n_0 k_a k_s (\beta \gamma \delta_1 \delta_2 A + \gamma^2 E_0^2)}{2\rho \epsilon \delta_3 (\Omega_a^2 + 2i\Gamma_a \omega_a)(\omega_0^2 - \omega_c^2 + 2iv\omega_0)} E_0 E_s^* \quad (16)$$

where $\Omega_a^2 = \omega_a^2 - k_a^2 v_a^2$, $\delta_3 = 1 - \frac{(\Omega_{ps}^2 - iv\omega_s)(\Omega_{pa}^2 + iv\omega_a)}{k_s^2 E^2}$,

in which $\Omega_{ps}^2 = \bar{\omega}_p^2 - \omega_s^2$, and $\Omega_{pa}^2 = \bar{\omega}_p^2 - \omega_a^2$.

The induced current density (J_{cd}) of the Brillouin medium at Stokes frequency (ω_s), including HCEs, is obtained (by neglecting transition dipole moment) as:

$$J_{cd}(\omega_s) = n_{1s}^* e v_0 = \frac{\epsilon_0 k_a k_s \omega_p^2 (v - i\omega_0)(\beta \gamma \delta_1 \delta_2 A + \gamma^2 E_0^2)}{2\rho \delta_3 (\Omega_a^2 + 2i\Gamma_a \omega_a)(\omega_0^2 - \omega_c^2 + 2iv\omega_0)} |E_0|^2 E_s^* \quad (17)$$

The nonlinear induced polarization of the Brillouin medium (which is time integral of induced current density), including HCEs, is obtained as:

$$P_{cd}(\omega_s) = \int J_{cd}(\omega_s) dt = \frac{\epsilon_0 k_a k_s \omega_p^2 \omega_0^3 (\beta \gamma \delta_1 \delta_2 A + \gamma^2 E_0^2)}{2\rho \omega_s \delta_3 (\Omega_a^2 + 2i\Gamma_a \omega_a)(\omega_0^2 - \omega_c^2 + 2iv\omega_0)} |E_0|^2 E_s^* \quad (18)$$

$$\text{Re}(\chi_B) = \frac{k_a k_s \omega_0^3 [\Omega_a^2 (\omega_0^2 - \omega_c^2) - 4v\Gamma_a \omega_a \omega_0] [\epsilon_0 \omega_p^2 (\beta \gamma \delta_1 \delta_2 A + \gamma^2 E_0^2) + \delta_3 \omega_s \omega_0 \gamma^2]}{2\rho \epsilon_0 \delta_3 \omega_s (\Omega_a^4 + 4\Gamma_a^2 \omega_a^2) [(\omega_0^2 - \omega_c^2)^2 + 4v^2 \omega_0^2]} \quad (22a)$$

$$\text{Im}(\chi_B) = -\frac{k_a k_s \omega_0^3 [v\omega_0 \Omega_a^2 + \Gamma_a \omega_a (\omega_0^2 - \omega_c^2)] [\epsilon_0 \omega_p^2 (\beta \gamma \delta_1 \delta_2 A + \gamma^2 E_0^2) + \delta_3 \omega_s \omega_0 \gamma^2]}{\rho \epsilon_0 \delta_3 \omega_s (\Omega_a^4 + 4\Gamma_a^2 \omega_a^2) [(\omega_0^2 - \omega_c^2)^2 + 4v^2 \omega_0^2]} \quad (22b)$$

Eqs. (22a) and (22b) show that both $\text{Re}(\chi_B)$ as well as $\text{Im}(\chi_B)$ are influenced by β , γ , n_0 (via ω_p), and B_0 (via ω_c). $\text{Im}(\chi_B)$ accounts for nonlinear absorption coefficient while $\text{Re}(\chi_B)$ is responsible for nonlinear refractive index of the chosen Brillouin medium. The knowledge of nonlinear absorption coefficient and refractive index of the Brillouin medium provide the information regarding the design of various optoelectronic devices including amplifiers, oscillators, filters, and couplers.

Besides $P_{cd}(\omega_s)$, the Brillouin medium also possesses a polarization $P_{es}(\omega_s)$ originating via electrostrictive property. Following Singh et al. (2008), and using Eqs. (1) and (5), we obtain

$$P_{es}(\omega_s) = \frac{k_a k_s \omega_0^4 \gamma^2}{2\rho (\Omega_a^2 + 2i\Gamma_a \omega_a)(\omega_0^2 - \omega_c^2 + 2iv\omega_0)} |E_0|^2 E_s^* \quad (19)$$

Using Eqs. (18) and (19), the effective nonlinear induced polarization of Brillouin medium, including HCEs, is given by

$$P(\omega_s) = P_{cd}(\omega_s) + P_{es}(\omega_s) = \frac{k_a k_s \omega_0^3 [\epsilon_0 \omega_p^2 (\beta \gamma \delta_1 \delta_2 A + \gamma^2 E_0^2) + \delta_3 \omega_s \omega_0 \gamma^2]}{2\rho \delta_3 \omega_s (\Omega_a^2 + 2i\Gamma_a \omega_a)(\omega_0^2 - \omega_c^2 + 2iv\omega_0)} |E_0|^2 E_s^* \quad (20)$$

Consequently, the effective Brillouin susceptibility of the Brillouin medium, including HCEs, is given by

$$\chi_B = \frac{k_a k_s \omega_0^3 [\epsilon_0 \omega_p^2 (\beta \gamma \delta_1 \delta_2 A + \gamma^2 E_0^2) + \delta_3 \omega_s \omega_0 \gamma^2]}{2\rho \epsilon_0 \delta_3 \omega_s (\Omega_a^2 + 2i\Gamma_a \omega_a)(\omega_0^2 - \omega_c^2 + 2iv\omega_0)} \quad (21)$$

Eq. (21) reveals that χ_B is a complex quantity and it can be put forward as: $\chi_B = \text{Re}(\chi_B) + i \text{Im}(\chi_B)$, where $\text{Re}(\chi_B)$ and $\text{Im}(\chi_B)$ stand for real and imaginary parts of complex χ_B , respectively. Rationalizing Eq. (21), we obtain

4. Results and discussion

In order to perform the numerical analysis, we choose n-type doped InSb crystal at 77K temperature as a Brillouin medium and illuminated it by a pulsed CO₂ laser at 10.6 μm wavelength. The absorption coefficient of chosen Brillouin medium is negligible at liquid nitrogen temperature around 10 μm wavelength and the effects of band-to-band transitions can be ignored safely (Toudert & Serna, 2017). The material parameters of n-InSb – CO₂ laser system are as follows (Singh et al., 2008): $m = 0.014m_0$; m_0 is the electron's rest mass, $\rho = 5.8 \times 10^3$

kg m^{-3} , $\epsilon = 17.8$, $\epsilon_\infty = 15.68$, $v_a = 4 \times 10^3 \text{ms}^{-1}$, $\beta = 0.054 \text{ Cm}^{-2}$, $\gamma = 5 \times 10^{10} \text{ s}^{-1}$, $\Gamma_a = 2 \times 10^{10} \text{ s}^{-1}$, $v_0 = 3.5 \times 10^{11} \text{ s}^{-1}$, $\omega_a = 2 \times 10^{11} \text{ s}^{-1}$, $\omega_0 = 1.78 \times 10^{14} \text{ s}^{-1}$, $T_0 = 77 \text{K}$, $\theta_D = 278 \text{K}$.

Eqs. (22a) and (22b) represent $\text{Re}(\chi_B)$ and $\text{Im}(\chi_B)$ of the Brillouin medium, respectively with including HCEs. The expression for $\text{Re}(\chi_B)$ and $\text{Im}(\chi_B)$ of the Brillouin medium with excluding HCEs can be obtained by simply replacing v by v_0 (at $T_e = T_0$) in these equations,

respectively. The dependence of $\text{Re}(\chi_B)$ and $\text{Im}(\chi_B)$ on external magnetic field B_0 (via ω_c) and doping concentration n_0 (via ω_p) with excluding and including HCEs are explored. Aim is targeted at: (i) determination of suitable values of B_0 and n_0 to enhance $\text{Re}(\chi_B)$ and $\text{Im}(\chi_B)$, and (ii) searching the usefulness of efficient optoelectronic devices based on Brillouin nonlinearities.

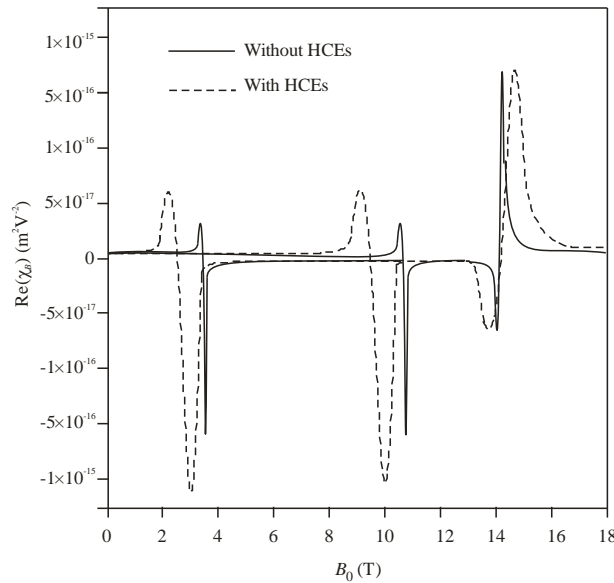


Figure 1a Plot of $\text{Re}(\chi_B)$ versus B_0 for the cases: (i) excluding HCEs, and (ii) including HCEs for $n_0 = 2 \times 10^{19} \text{ m}^{-3}$ and $E_0 = 7 \times 10^7 \text{ Vm}^{-1}$.

In Figures 1a and 1b, $\text{Re}(\chi_B)$ and $\text{Im}(\chi_B)$ are plotted versus B_0 , respectively for the cases: (i) excluding HCEs, and (ii) including HCEs. These clearly show the substantial enhancements of $\text{Re}(\chi_B)$ and $\text{Im}(\chi_B)$ as well as alter of their sign. The situation at which $\text{Re}(\chi_B)$ and $\text{Im}(\chi_B)$ alter their sign is termed as ‘cut-off’ or ‘dielectric anomaly’ (Palik & Furdyna, 1970).

When HCEs are excluded, with rising B_0 , $\text{Re}(\chi_B)$ is positive while $\text{Im}(\chi_B)$ is negative, vanishingly small, and remain independent of magnetic field for $0 \leq B_0 \leq 2.5 \text{ T}$. The nature of the curves of both $\text{Re}(\chi_B)$ and $\text{Im}(\chi_B)$ are very sensitive in the regime $2.5 \text{ T} < B_0 < 4.5 \text{ T}$. In this regime, with rising B_0 , $\text{Re}(\chi_B)$ starts increasing

while $\text{Im}(\chi_B)$ starts decreasing achieving a peak positive value ($\text{Re}(\chi_B) = 3 \times 10^{-17} \text{ m}^2 \text{V}^{-2}$) and a peak negative value ($\text{Im}(\chi_B) = -6 \times 10^{-17} \text{ m}^2 \text{V}^{-2}$), respectively at $B_0 = 3.4 \text{ T}$. With slightly rising B_0 beyond this value, $\text{Re}(\chi_B)$ starts sharply decreasing while $\text{Im}(\chi_B)$ starts sharply increasing. At $B_0 = 3.5 \text{ T}$, both $\text{Re}(\chi_B)$ and $\text{Im}(\chi_B)$ vanish. With further slightly rising B_0 beyond this value, both $\text{Re}(\chi_B)$ and $\text{Im}(\chi_B)$ alter their sign achieving a peak negative value ($\text{Re}(\chi_B) = -6 \times 10^{-16} \text{ m}^2 \text{V}^{-2}$) and peak positive value ($\text{Im}(\chi_B) = 2 \times 10^{-15} \text{ m}^2 \text{V}^{-2}$), respectively at $B_0 = 3.6 \text{ T}$. For $3.6 \text{ T} < B_0 < 4.5 \text{ T}$, $\text{Re}(\chi_B)$ increases sharply while $\text{Im}(\chi_B)$ decreases sharply. For $4.5 \text{ T} \leq B_0 \leq 10 \text{ T}$, $\text{Re}(\chi_B)$ remains negative

while $\text{Im}(\chi_B)$ remains positive and vanishingly small. The nature of the curves of both $\text{Re}(\chi_B)$ and $\text{Im}(\chi_B)$ is again repeated in the regime $10.8\text{T} < B_0 < 11.8\text{T}$ like the regime $2.5\text{T} < B_0 < 4.5\text{T}$. For the regime $11.8\text{T} \leq B_0 \leq 13.2\text{T}$, $\text{Re}(\chi_B)$ remains negative while $\text{Im}(\chi_B)$ remains positive and vanishingly small. This distinct behavior of $\text{Re}(\chi_B)$ and $\text{Im}(\chi_B)$ occur due to following resonance conditions: (i) $(\omega_p^2 \omega_c^2) / v^2 \sim \omega_s^2$, and (ii) $v^2 \omega_p^2 / (v^2 + \omega_c^2) \sim \omega_s^2$. An important aspect of these resonance conditions is the interaction between electron-plasmon mode and electron-cyclotron mode. Let we define this as coupled plasmon-cyclotron mode. When the laser radiation field interacts with this coupled mode, as a consequence, the coupled mode frequency dependent

Stokes mode is generated. Here, it is beneficial to shift the scattered Stokes mode frequency to an achievable spectral regime in proportion to ω_p (or n_0) for fixed ω_c (or B_0), ω_c (or B_0) for fixed ω_p (or n_0), and combination of ω_c and ω_p both. By continuously increasing n_0 (via ω_p) and decreasing B_0 (via ω_c) in the same proportion maintains the resonance conditions at a fixed value of ω_s . Further, by continuously increasing n_0 and decreasing B_0 without maintaining their proportion shifts the value of ω_s . At $B_0 = 14.2\text{T}$, the change of sign of both $\text{Re}(\chi_B)$ and $\text{Im}(\chi_B)$ is observed due to resonance condition: (iii) $\omega_c^2 \sim \omega_0^2$. This resonance condition is independent of ω_p (or n_0).

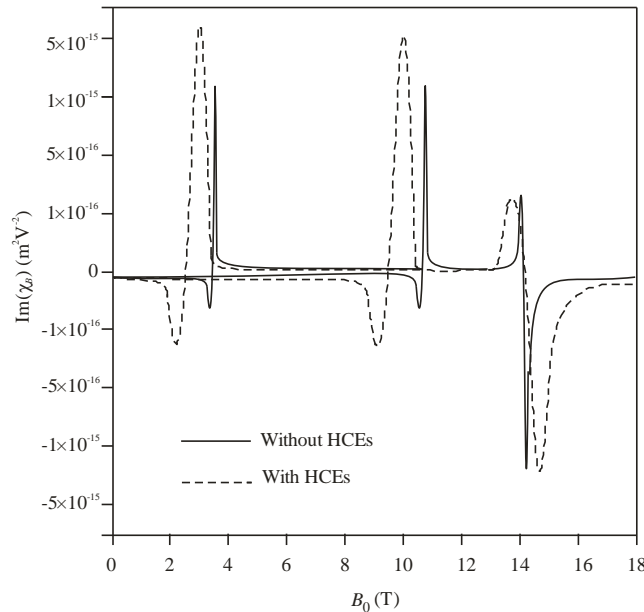


Figure 1b Plot of $\text{Im}(\chi_B)$ versus B_0 for the cases (i), (ii) and parameters given in Figure 1a.

When HCEs are included, the features of $\text{Re}(\chi_B) - B_0$ and $\text{Im}(\chi_B) - B_0$ plots remain unchanged except that:

1. the change of sign of $\text{Re}(\chi_B)$ and $\text{Im}(\chi_B)$ which was occurring at $B_0 = 3.5\text{T}$ and 10.8T is now shifted to $B_0 = 2.5\text{T}$ and 9.8T , respectively;
2. the peak positive and negative values of $\text{Re}(\chi_B)$ and $\text{Im}(\chi_B)$ occurring due to resonance conditions (i) and (ii) is enhanced almost five times;
3. the range of B_0 at which the change of sign of $\text{Re}(\chi_B)$ and $\text{Im}(\chi_B)$ occurs is widened.

4. The magnitude of $\text{Re}(\chi_B)$ and $\text{Im}(\chi_B)$ remain unaltered at resonance condition (iii) with including HCEs; rather this resonance condition shifts the value of B_0 at which resonance occurs towards lower values and widens the range of B_0 at which change of sign of both $\text{Re}(\chi_B)$ and $\text{Im}(\chi_B)$ occur.

Around resonances, the electron's drift velocity (which is the function of B_0) increases, attains a value higher than acoustical vibrational mode and due to this the rate of energy flow from laser radiation field to acoustical vibrational mode increases, and

consequently the amplification of acoustical vibrational mode takes place in the Brillouin medium. Eventually, the interaction between laser radiation field and

amplified acoustical vibrational mode enhances the amplitude of scattered Stokes mode.

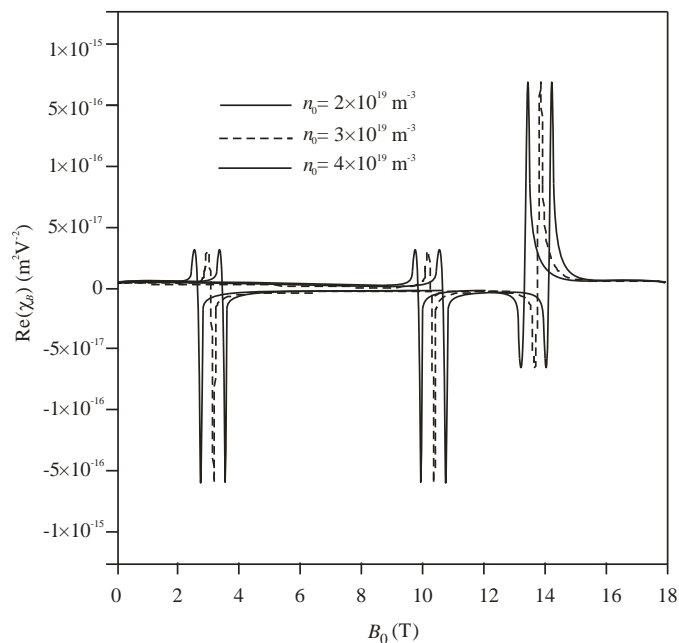


Figure 2a Plot of $\text{Re}(\chi_B)$ versus B_0 with excluding HCEs for three different doping concentration ($n_0 = 2 \times 10^{19} \text{ m}^{-3}$, $3 \times 10^{19} \text{ m}^{-3}$ and $n_0 = 4 \times 10^{19} \text{ m}^{-3}$) at $E_0 = 7 \times 10^7 \text{ Vm}^{-1}$.

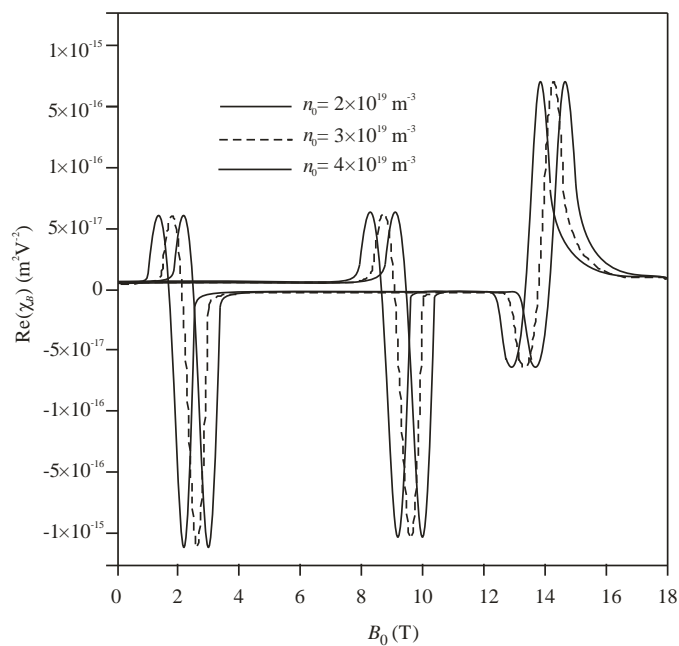


Figure 2b Plot of $\text{Re}(\chi_B)$ versus B_0 with including HCEs for the parameters given in Figure 2a.

The most significant feature of the results obtained is the monitoring of $\text{Re}(\chi_B)$ and $\text{Im}(\chi_B)$ by properly selecting B_0 and also attaining large values of $\text{Re}(\chi_B)$ and $\text{Im}(\chi_B)$ in a Brillouin medium consisting of semiconductor magneto-plasmas. The results obtained in Figures 1a and 1b permit the tuning of scattered Stokes mode over a broad frequency regime and open up the opportunity of fabrication of frequency converters.

The magnetic field considered in the present numerical analysis ($0 \leq B_0 \leq 18\text{T}$) is easily attainable in the laboratory. It should be worth pointing out that Generazio and Spector (1979) studied the free carrier absorption for n-InSb – CO₂ and n-InSb – CO laser systems at 77 K by placing the sample in an external magnetic field $B_0 \leq 20\text{T}$.

In Figures 2a and 2b, $\text{Re}(\chi_B)$ is plotted versus magnetic field B_0 with excluding and including HCEs, respectively for three different doping concentration ($n_0 = 2 \times 10^{19}\text{ m}^{-3}$, $3 \times 10^{19}\text{ m}^{-3}$ and $n_0 = 4 \times 10^{19}\text{ m}^{-3}$) at $E_0 = 7 \times 10^7\text{ Vm}^{-1}$. These give a picture of the enhancement of $\text{Re}(\chi_B)$ as well as alter of its signs. For a fixed n_0 , the nature of curves are similar to as obtained in Figure 1a. An increase in n_0 does not alters the magnitude of peak

positive and negative values of $\text{Re}(\chi_B)$, rather it shifts the value of B_0 , at which change of sign of $\text{Re}(\chi_B)$ occurs, towards lower values. A comparison between results of Figures 2a and 2b reveals that for a fixed n_0 , the HCEs induced by laser radiation widens the range of B_0 at which the change of sign of $\text{Re}(\chi_B)$ occurs; a result which supports the results of Figure 1a.

In Figures 3a and 3b, $\text{Im}(\chi_B)$ is plotted versus magnetic field B_0 with excluding and including HCEs, respectively for the parameters given in Figures 2a and 2b. These give a picture of the enhancement of $\text{Im}(\chi_B)$ as well as alter of its signs. For a fixed n_0 , the nature of curves are similar to as obtained in Figure 1b. An increase in n_0 does not alters the magnitude of peak positive and negative values of $\text{Im}(\chi_B)$, rather it shifts the value of B_0 , at which change of sign of $\text{Im}(\chi_B)$ occurs, towards lower values. A comparison between results of Figures 3a and 3b reveals that for a fixed n_0 , the HCEs induced by intense laser radiation widens the range of B_0 at which the change of sign of $\text{Im}(\chi_B)$ occurs; a result which supports the results of Figure 1b.

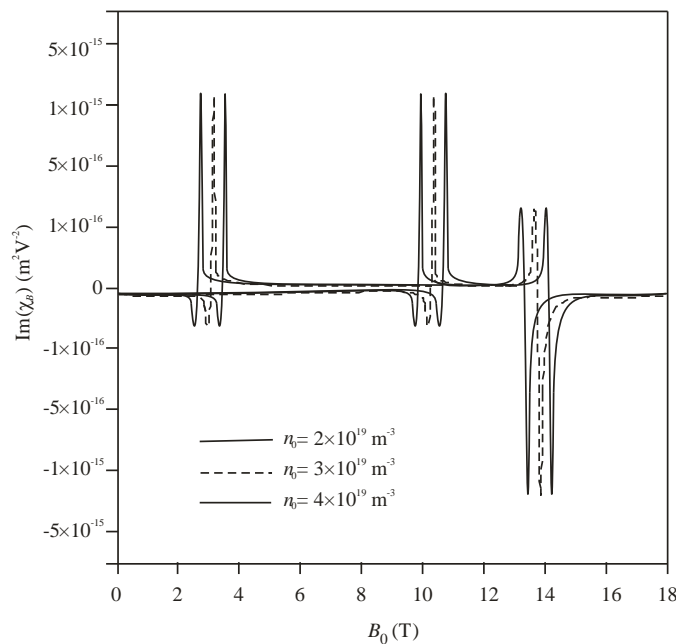


Figure 3a Plot of $\text{Im}(\chi_B)$ versus B_0 with excluding HCEs for the parameters given in Figure 2a.

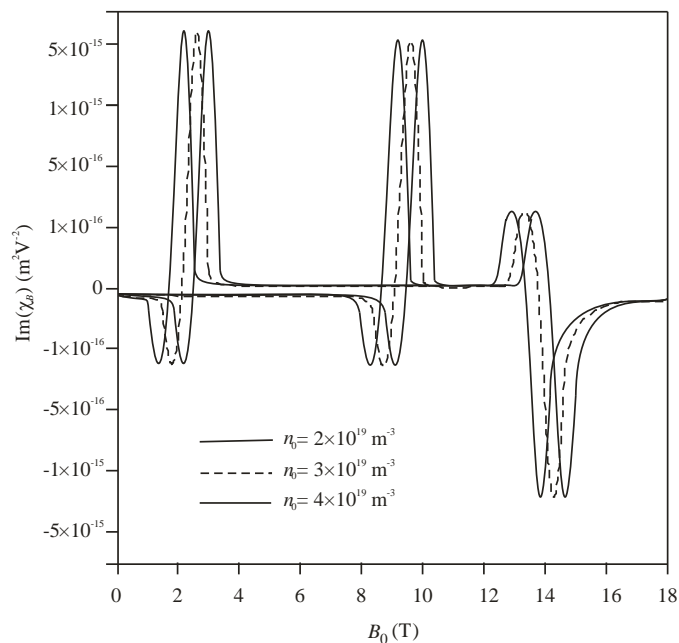


Figure 3b Plot of $\text{Im}(\chi_B)$ versus B_0 with including HCEs for the parameters given in Figure 2a.

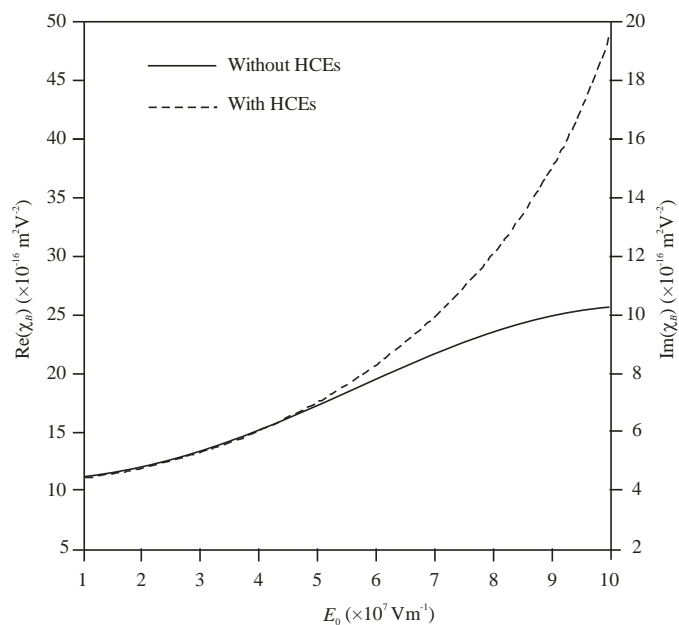


Figure 4 Plot of $\text{Re}, \text{Im}(\chi_B)$ versus E_0 at $B_0 \approx 14.2$ T for the cases (i) and (ii) given in Figure 1a.

From Eqs. (22a) and (22b), it can be seen that apart from magnetic field dependence, laser radiation field strength can also be employed to enhance $\text{Re}(\chi_B)$ and $\text{Im}(\chi_B)$. In Figure 4, both $\text{Re}(\chi_B)$ and $\text{Im}(\chi_B)$ are plotted versus laser radiation field amplitude E_0 for the cases: (i) excluding HCEs, and

(ii) including HCEs. It can be seen that both $\text{Re}(\chi_B)$ and $\text{Im}(\chi_B)$ exhibit the similar nature of curves throughout the plotted range of E_0 such that $\text{Re}(\chi_B) = 2.5 \text{Im}(\chi_B)$. When HCEs are included, the shape of the curve is a parabola. For smaller values of $E_0 (< 4 \times 10^7 \text{ Vm}^{-1})$ when HCEs are

insignificant, both $\text{Re}(\chi_B)$ and $\text{Im}(\chi_B)$ increases in a parabolic shape with increasing E_0 . However, they gradually start deviating from the parabolic shape as HCEs become significant, in the region $E_0 \geq 4 \times 10^7 \text{ Vm}^{-1}$. Both $\text{Re}(\chi_B)$ and $\text{Im}(\chi_B)$ become almost independent of E_0 beyond $E_0 \approx 10^8 \text{ Vm}^{-1}$ and as evident from this figure that both $\text{Re}(\chi_B)$ and $\text{Im}(\chi_B)$ become almost double when HCEs are included in comparison to when they are excluded. This behaviour can be easily understood in terms of temperature dependence of $\text{Re}(\chi_B)$ and $\text{Im}(\chi_B)$ via MTCF of electrons in Eqs. (22a) and (22b), respectively. This deviation of real and imaginary parts of Brillouin susceptibility curves (from the parabolic shape), at high laser radiation field emphasis the necessity of inclusion of HCEs in SBS processes.

5. Conclusions

In the present paper, a theoretical formulation followed by numerical analysis is made to study HCEs on real and imaginary parts of Brillouin susceptibility of semiconductor magneto-plasmas. The analysis enables one to draw the following conclusions:

1. The semiconductors fluid model is used very fruitfully to study the influence of HCEs of intense laser radiation on $\text{Re}(\chi_B)$ and $\text{Im}(\chi_B)$ of semiconductor magneto-plasmas.
2. The analysis offer three achievable resonance conditions: (i) $(\omega_p^2 \omega_c^2) / v^2 \sim \omega_s^2$, (ii) $v^2 \omega_p^2 / (v^2 + \omega_c^2) \sim \omega_s^2$, and (iii) $\omega_c^2 \omega_0^2$ at which significant enhancement as well as change of sign of both $\text{Re}(\chi_B)$ and $\text{Im}(\chi_B)$ occur. Resonance conditions (i) and (ii) offer the tuning of scattered Stokes Brillouin mode over a wide frequency regime by proper selection of the doping level and/or external magnetic field.
3. The HCEs of intense laser radiation: (a) enhances the peak positive and negative values of $\text{Re}(\chi_B)$ and $\text{Im}(\chi_B)$ considerably, (b) shifts the enhanced peak positive and negative values of $\text{Re}(\chi_B)$ and $\text{Im}(\chi_B)$ towards lower values of magnetic field, and (c) widens the range of magnetic field at which the change of sign of $\text{Re}(\chi_B)$ and $\text{Im}(\chi_B)$ occur.
4. For laser radiation field amplitude $E_0 < 4 \times 10^7 \text{ Vm}^{-1}$, HCEs on $\text{Re}, \text{Im}(\chi_B)$ are absent.

However, for $E_0 \geq 4 \times 10^7 \text{ Vm}^{-1}$, HCEs become significant and more pronounced.

5. The technological potentiality of semiconductor magneto-plasmas as the hosts for the fabrication of SBS dependent widely tunable and efficient optoelectronic devices such as optical switches and frequency converters.

6. Acknowledgements

We are thankful to Prof. S.K. Ghoshal, Department of Physics, Universiti Teknologi, Malaysia for many useful suggestions to carry out this work.

7. References

- Bai, Z., Yuan, H., Liu, Z., Xu, P., Gao, Q., Williams, R. J., ... & Lu, Z. (2018). Stimulated Brillouin scattering materials, experimental design and applications: A review. *Optical Materials*, 75, 626-645. DOI: 10.1016/j.optmat.2017.10.035
- Beer, A. C. (1963). *Galvanometric Effects in Semiconductors: Solid State Physics*. New York, USA: Academic Press.
- Bhan, S., Singh, H. P., Kumar, V., & Singh, M. (2019). Low threshold and high reflectivity of optical phase conjugate mode in transversely magnetized semiconductors. *Optik*, 184, 467-472. DOI: 10.1016/j.ijleo.2019.04.106
- Chefranov, S. G., & Chefranov A. S. (2020). Hydrodynamic Methods and Exact Solutions in Applications to the Electromagnetic Field Theory in Medium. In: *Nonlinear Optics – Novel Results in Field Theory in Medium*. Lembrikov B. (ed.). UK: Intechopen.
- Conwell, E. M. (1967). *High Field Transport in Semiconductors*. New York, USA: Academic Press, pp. 159.
- Garmire, E. (2017). Prospectives on stimulated Brillouin scattering. *New Journal of Physics*, 19, 011003. DOI: 10.1088/1367-2630/aa5447
- Garmire, E. (2018). Stimulated Brillouin review: invented 50 years ago and applied today. *International Journal of Optics*, 2018, Article ID 2459501. DOI: 10.1155/2018/2459501
- Generazio, E. R., & Spector, H. N. (1979). Free-

- carrier absorption in quantizing magnetic fields. *PhysicalReview B*, 20, 5162-5167. DOI: 10.1103/PhysRevB.20.5162
- Hass, F., & Bret, A. (2012). Nonlinear low-frequency collisional quantum Buneman instability, *Europhysics Letters*, 97(2), 26001. DOI: 10.1209/0295-5075/97/26001
- Lu, Y., Zhang, Q., Wu, Q., Chen, Z., & Xu, J. (2021). Giant enhancement of THz-frequency optical nonlinearity by phonon polariton in ionic crystals. *Nature Communications*, 12, 3183. DOI: 10.1038/s41467-021-23526-w
- Moghanjoughi, M. A. (2011). Nonlinear ion waves in Fermi-Dirac pair plasmas. *Physics of Plasmas*, 18(1), 012701. DOI: 10.1063/1.3533425
- Mokkapati, S., & Jagadish, C. (2009). III-V compound SC for optoelectronic devices. *Materialstoday*, 12(4), 22-32. DOI: 10.1016/S1369-7021(09)70110-5
- Nimje, N., Dubey, S., & Ghosh, S. (2011). Parametric interaction in acousto-optical semiconductor plasmas in the presence of hot carriers. *Chinese Journal of Physics-Taipei*, 49(4), 901-916.
- Palik, E. D., & Furdyna, J. K. (1970). Infrared and microwave magnetoplasma effects in semiconductors. *Reports on Progress in Physics*, 33(3), 1193-1322. DOI: 10.1088/0034-4885/33/3/307
- Rasheed, A., Jamil, M., Siddique, M., Huda, F., & Jung, Y. D. (2014). Beam excited acoustic instability in semiconductor quantum plasmas. *Physics of Plasmas*, 21(6), 062107. DOI: 10.1063/1.4883224
- Sandeep, D., S., & Singh, N. (2017). Parametric excitation of optical phonons in weakly polar narrow band gap magnetized semiconductor plasmas. *Modern Physics Letters B*, 31(31), 1750294. DOI: 10.1142/S0217984917502943
- Säynätjoki, A., Karvonen, L., Rostami, H., Autere, A., Mehrovar, S., Lombardo, A., ... & Sun, Z. (2017). Ultra-strong nonlinear optical processes and trigonal warping in MoS₂ layers. *Nature communications*, 8(1), 1-8. DOI: 10.1038/s41467-017-00749-4
- Sharaf, E. R., Mohammed, M. I., Zahran, H. Y., & Shaaban, E. R. (2021). High refractive index and third-order nonlinear optical susceptibility of nanostructured ZnSe/FTO thin films: towards smart multifunctional optoelectronic materials. *Physica B Condensed Matter*, 602, 412595. DOI: 10.1016/j.physb.2020.412595
- Sharma, G., & Ghosh, S. (2001). Parametric excitation and amplification of an acoustic wave in a magnetised piezoelectric semiconductor. *physica status solidi (a)*, 184(2), 443-452. DOI: 10.1002/1521-396X(200104)184:2<443::AID-PSSA443>3.0.CO;2-S
- Sharma, G., Dad, R. C., & Ghosh, S. (2015). Stimulated Brillouin scattering of laser in semiconductor plasma embedded with nano-sized grains. *AIP Conference Proceedings*, 1670, 0300026. DOI: 10.1063/1.4926710
- Singh, M., Aghamkar, P., Kishore, N., & Sen, P. K. (2006). Influence of piezoelectricity and magnetic field on stimulated Brillouin scattering in III-V semiconductors. *Journal of Nonlinear Optical Physics & Materials*, 15(4), 465-479. DOI: 10.1142/S0218863506003487
- Singh, M., & Aghamkar, P. (2008). Mechanism of phase conjugation via stimulated Brillouin scattering in narrow bandgap semiconductors. *Optics Communications*, 281(5), 1251-1255. DOI: <https://doi.org/10.1016/j.optcom.2007.10.102>
- Singh, M., Aghamkar, P., Kishore, N., & Sen, P. K. (2008). Nonlinear absorption and refractive index of Brillouin scattered mode in semiconductor-plasmas by an applied magnetic field. *Optics and Laser Technology*, 40(1), 215-222. DOI: 10.1016/j.optlastec.2007.02.001
- Singh, M., Gahlawat, J., Sangwan, A., Singh, N., & Singh, M. (2020). Nonlinear optical susceptibilities of a piezoelectric semiconductor magneto-plasma. *Springer Proceedings in Physics*, 256, 189-202, ch. 20 (2020). DOI: 10.1007/978-981-15-8625-5_20
- Sodha, M. S., Ghatak, A. K., & Tripathi, V. K. (1974). Self-focusing of laser beams in dielectrics, plasmas and semiconductors.

- New Delhi, India: Tata McGraw, pp. 55-62.
- Takeya, K., Kamei, T., Kawase, K., & Uchida, H. (2020). Nonlinear optical processes of second-order nonlinear optical susceptibility $\chi^{(2)}_{133}$ in an organic nonlinear optical crystal DAST. *Optics Letters*, 45(19), 5348-5351. DOI: 10.1364/OL.400235
- Toudert, J., & Serna, R. (2017). Interband transitions in semi-metals, semiconductors, and topological insulators: a new driving force for plasmonics and nanophotonics. *Optical Materials Express*, 7(7), 2299-2325. DOI: 10.1364/OME.7.002299
- Tuz, V. R., Fesenko, V. I., Fedorin, I. V., Sun, H. B., & Han, W. (2017). Coexistence of bulk and surface polaritons in a magnetic-semiconductor superlattice influenced by a transverse magnetic field. *Journal of Applied Physics*, 121(10), 103102. DOI: 10.1063/1.4977956
- Uzma, C., Zeba, I., Shah, H. A., & Salimullah, M. (2009). Stimulated Brillouin scattering of laser radiation in a piezoelectric semiconductor: quantum effect. *Journal of Applied Physics*, 105(1), 013307. DOI: 10.1063/1.3050340
- Vanshpal, R., Dubey, S., & Ghosh, S. (2013). Stimulated Brillouin scattering in semiconductors: Quantum effects, *AIP Conference Proceedings*, 1535(1), 335. DOI: 10.1063/1.4810237
- Wang, K., Seidel, M., Nagarajan, K., Chervy, T., Genet, C., & Ebbesen, T. (2021). Large optical nonlinearity enhancement under electronic strong coupling. *Nature Communications*, 12(1), 1486. DOI: 10.1038/s41467-021-21739-7
- You, J. W., Bongu, S. R., Bao, Q., & Panoiu, N. C. (2018). Nonlinear optical properties and applications of 2D materials: theoretical and experimental aspects. *Nanophotonics*, 8(1), 63-97. DOI: 10.1515/nanoph—2018-0106